Synthetic Biology, 2025, **10(1)**, ysaf004
DOI: https://doi.org/10.1093/synbio/ysaf004
Advance Access Publication date: 4 April 2025
Research Article

Two highly specific growth-coupled biosensor for glycolaldehyde detection across micromolar and millimolar concentrations

Paul A. Gómez-Coronado[1,2], Armin Kubis[2], Maria Kowald[2], Rahma Ute[2], Charlie Cotton[2], Steffen N. Lindner[2,3], Arren Bar-Even[2,†], Tobias J. Erb[1,4,*]

[1]Department of Biochemistry and Synthetic Metabolism,Max Planck Institute for Terrestrial Microbiology, Karl-von-Frisch-Str. 10, Marburg, Hessen 35043, Germany
[2]Research Group Systems and Synthetic Metabolism,Max Planck Institute of Molecular Plant Physiology, Am Mühlenberg 1, Potsdam-Golm, Brandenburg 14476, Germany
[3]Department of Biochemistry, Charité Universitätsmedizin Berlin, Freie Universität Berlin and Humboldt-Universität, Berlin, Charitéplatz 1, Berlin 10117, Germany
[4]Center for Synthetic Microbiology (SYNMIKRO), Philipps University Marburg, Karl-von-Frisch-Str. 14, Marburg, Hessen 35043, Germany
[†]Deceased in September 2020.
* Corresponding author. Department of Biochemistry and Synthetic Metabolism,Max Planck Institute for Terrestrial Microbiology, Karl-von-Frisch-Str. 10, Marburg, Hessen 35043, Germany. E-mail: toerb@mpi-marburg.mpg.de

Abstract

Glycolaldehyde (GA), the smallest sugar, has significant potential as a biomass-derived platform chemical and is a key metabolite in several synthetic pathways for one-carbon metabolism and new-to-nature photorespiration. This study introduces two metabolic schemes for engineering *Escherichia coli* into GA biosensors. Through creating GA-dependent auxotrophies, we link growth of these strains to GA-dependent biosynthesis of the essential vitamin pyridoxal-5-phosphate, and 2-ketoglutarate, respectively. We characterized and optimized these strains for the quantification of externally added GA from 2 μM to 1.5 mM. We also demonstrate the capability of these strains to detect GA that is produced intracellularly through different metabolic routes and from different substrates such as xylose, ethylene glycol, and glycolate. Our biosensors offer complementary sensitivities and features, opening up different applications in metabolic engineering and synthetic biology, which we demonstrate in a proof-of-principle by providing the first *in vivo* demonstration of the reduction of glycolate to GA by a new-to-nature route using engineered enzymes.

Keywords: microbial biosensor; glycolaldehyde detection; ethylene glycol; synthetic metabolism

Graphical Abstract

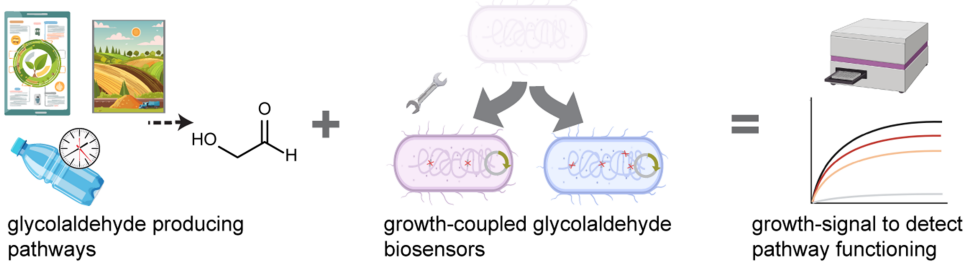

Introduction

Glycolaldehyde (GA), by definition the smallest sugar, holds promise as a future biomass-derived platform chemical. While directly used in the food industry as browning agent [1], GA is also the starting point for a variety of industrially relevant compounds such as alkanol amines and ethylene diamines, which showcases its versatility as chemical building block [2]. In addition, GA is an intermediate in the (bio)synthesis of valuable C2 and C4 molecules, such as ethylene glycol, glycolic acid, and D-erythrose [3, 4].

GA can be generated from non-fossil sources like xylose [3, 4], as well as through the breakdown of polyethylene terephthalate

Submitted: 27 February 2025; **Received (in revised form)**: 30 January 2025; **Accepted**: 3 April 2025

(PET) plastics, where it is derived from the PET building block ethylene glycol [5]. In addition, several new-to-nature pathways for the formation of GA from carbon dioxide or methanol have been described recently, which rely on an engineered glycolaldehyde synthase [6, 7]. Beyond these pathways, GA has also been identified as a key metabolite in various alternative photorespiration routes, where it is formed during recycling of glycolate, a photorespiratory waste product [8]. Four of the five most promising synthetic photorespiration pathways rely on the non-natural reduction of glycolate to GA via engineered enzymes, specifically a glycolyl-CoA synthetase (GCS) and a glycolyl-CoA reductase (GCR). These two enzymes showed activity *in vitro* and GCS was further improved in a follow-up study, recently [9].

The pivotal role of GA has raised the demand for sensing the compound *in vivo*. Prior work led to the development of a plasmid-based *Escherichia coli* biosensor for aldehydes, including GA, by Frazão et al. This biosensor functions through the upregulation of a transcription regulator upon aldehyde exposure [10]. However, the broad sensitivity of the biosensor and the lack of GA specificity have increased the need for more targeted biosensor development.

Here, we combined metabolic engineering and synthetic biology to develop two highly specific GA *E. coli* sensor strains [11]. The growth of these strains is linked to the GA-dependent biosynthesis of the essential vitamin pyridoxal-5-phosphate (PLP), or the biomass precursors 2-ketoglutarate (2KG), respectively. We characterized and optimized these strains for sensing GA and validated their capability to detect externally added GA, as well as GA that was produced intracellularly from various substrates, including xylose, ethylene glycol, and glycolate. We further demonstrate that these strains provide complementary sensitivity and features and can be used for different applications in synthetic biology and metabolic engineering.

Material and methods

Chemicals were ordered from Sigma-Aldrich (Steinheim, Germany), Tokyo Chemical Industry (Eschborn, Germany), and Carl Roth (Karlsruhe, Germany).

Generation of sensor strains

For this study, we used *E. coli* K12 WT strains SIJ488 and their derivatives. The SIJ488 strain is engineered with inducible λ-Red recombineering genes (Red-recombinase and flippase) integrated into its genome, facilitating multiple gene deletions [12]. Gene deletions were performed using the RedE and RedT technique [13]. In this method, PCR was used to generate linear DNA fragments with 50-bp homology arms targeting the gene of interest, along with a selectable marker for Kanamycin (Kan) or Chloramphenicol (CAP) resistance. These fragments were created using either the FRT-PGKgb2-neo-FRT cassette (Gene Bridges, Germany) or the pKD3 plasmid [14] as templates.

Approximately 400 ng of these DNA fragments were introduced into freshly cultured parental strains at an OD_{600} of ∼0.3, following the induction of recombinase enzymes with 15 mM L-Arabinose for 45 min. Selection of strains with the new deletions was performed by culturing on the appropriate antibiotics (Kan/CAP) and verifying through PCR to assess the size of the altered genomic locus.

Alternatively, single gene deletion strains from the "Keio collection" [15] were used to create phage lysates and transduce desired deletion combinations [16].

To chromosomally integrate *C. crecentus* genes *Cc_xylX* and *Cc_xylA* into the 2KG-aux strain. We first constructed single gene carrying vectors for propagation: pNiv-B-*Cc_xylX* and pNiv-B-*Cc_xylA*. We then constructed via Gibson assembly a vector containing the operon pNiv-B-Cc_xylX-B-xylA preceded by a strong promotor using plasmid pKD3 as template for backbone. This was followed by creating a linear integration cassette consisting of the full operon flanked with upstream and downstream overhangs, of the intended insertion site, which was added with overlap PCR. For the integration of S-B-Cc_xylX-B-Cc_xylA into safe spot #9 (SS9) [17], the left and right integration overhang were amplified from pKD3 rbsB xylX rbsB xylA using primers pKD_knock-in_SS9_F + pKD_knock-in_SS9_R, respectively. The Knock-In cassette obtained was then used electroporated as described before for deletions by λ-Red recombineering.

Similarly, for thrB integration in SS9 of PLP-aux strain, we created an integration cassette using a plasmid containing the expression unit of thrB flanked by upstream and downstream overhangs of SS9 as template (pDM4-SS9-S-C-thrB) with primers pDM4-Linear-SS9_F + pDM4-Linear-SS9_R. We then proceeded same as described earlier for deletions by λ-Red recombineering.

Resistance genes for kanamycin or chloramphenicol were integrated into the genome, flanked by FRT sites in place of the target gene (in case of deletions), or downstream of the expression unit to be integrated. To excise the selectable marker before further engineering of the strains, flippase was induced in a culture at an OD_{600} of ∼0.2 by adding 50 mM L-rhamnose and incubating for ∼4 h at 30°C. The removal of antibiotic resistance was confirmed by isolating colonies that could only proliferate on LB medium without the respective antibiotic and by PCR analysis of the genomic locus.

All strains used in this study are listed in Supplementary Table 1. NEB5α cells were utilized for cloning. For overexpression purposes, plasmids described in the following section were introduced into the relevant strains through electroporation.

Expression vectors

Primers were synthesized by Eurofins (Ebersberg, Germany) and Sigma-Aldrich (Steinheim, Germany). PCR reactions were performed using PrimeSTAR GXL DNA Polymerase (Clontech, Heidelberg, Germany), Phusion DNA Polymerase (Thermo Fisher Scientific, Dreieich, Germany), and DreamTaq DNA Polymerase (Thermo Fisher Scientific, Dreieich, Germany). Restrictions were carried out using FastDigest enzymes and ligations using T4 DNA ligase, all purchased from Thermo Fisher Scientific (Dreieich, Germany).

For plasmid-based gene overexpression, the pZ-AS(S or M) plasmid (p15A origin of replication and strong or medium promoter [18] were used. Gene coding for the CoA-transferase (*abfT*) from *Clostridium aminobutyricum* (UniProt ID Q9RM86) and each gene of the xylose utilization operon (xylBCDXA, *C. crescentus* NA1000) were codon optimized for *E. coli* (strain K12) via Jcat [19] and synthesized by Twist Bioscience (USA). *Escherichia coli* enzyme L-1,2-propanediol oxidoreductase (FucO) was amplified from the genome with the introduction of two mutations (I7L and L8V) that were reported to increase its resistance to metal-catalyzed oxidation [20]. Operons were then constructed according to previously described method [18]. After cloning steps were completed, NEB5α cells were transformed with the product for cryopreservation. Successful plasmid assembly was confirmed by whole-plasmid sequencing (Plasmidsaurus, USA) or Sanger sequencing (Microsynth Seqlab GmbH, Germany).

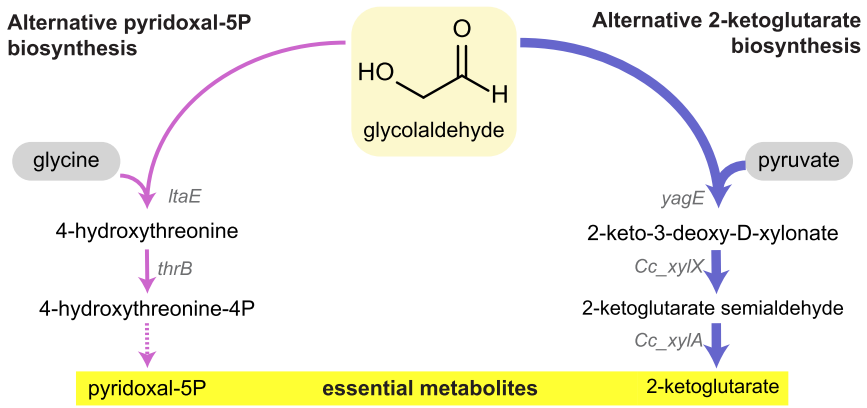

Figure 1. Glycolaldehyde-dependent biosynthesis of essential metabolites. Alternative PLP biosynthesis. Aldol condensation of GA and glycine is catalyzed by the low-specificity threonine aldolase (LtaE). 4-Hydroxythreonine is phosphorylated by homoserine kinase (ThrB). 4-Hydroxythreonine-4P is intermediate of canonical PLP biosynthesis (dashed line) which leads to essential metabolite PLP. Alternative 2KG biosynthesis. 2-Dehydro-3-deoxy-D-pentonate (YagE) drives the aldol condensation of GA and pyruvate. 2-Keto-3-deoxy- D-xylonate is converted by *C. crescentus* *Cc_xylX* and *Cc_xylA* to 2KG.

Growth media

Escherichia coli strains were routinely cultured in LB medium (comprising 5 g/l yeast extract, 10 g/l tryptone, and 10 g/l NaCl), at a temperature of 37°C and a shaking speed of 220 – 250 rpm. Antibiotics were added as necessary at the following concentrations: kanamycin at 50 μg/ml; chloramphenicol at 30 μg/ml (prepared as a 1000X stock solution in 70% ethanol); and streptomycin at 100 μg/ml. Antibiotics were omitted for growth experiments, with the exception of their use in precultures. Growth assays utilized M9 minimal medium (containing 47.8 mM Na_2HPO_4, 22 mM KH_2PO_4, 8.6 mM NaCl, 18.7 mM NH_4Cl, 2 mM $MgSO_4$, and 100 μM $CaCl_2$), enriched with trace elements (134 μM EDTA, 31 μM $FeCl_3 \cdot 6H_2O$, 6.2 μM $ZnCl_2$, 0.76 μM $CuCl_2 \cdot 2H_2O$, 0.42 μM $CoCl_2 \cdot 2H_2O$, 1.62 μM H_3BO_3, and 0.081 μM $MnCl_2 \cdot 4H_2O$). Carbon sources and additional supplements were added based on the specific requirements of each strain and the nature of the experiment. Precultures for growth assays were cultivated in M9 medium under identical conditions and using the same carbon source as would later be employed for the control group under "positive control". Cells from these precultures were washed three times in M9 medium devoid of carbon sources and then inoculated into M9 media with selected carbon sources at a starting OD_{600} of 0.005. Nunc 96-well microplates (Thermo Fisher Scientific) were utilized for the growth experiments, with each well containing 150 μl of culture and overlaid with 50 μl of mineral oil (Sigma-Aldrich) to prevent evaporation.

The growth experiments were conducted using either a Tecan Infinite 200 Pro plate reader (Tecan, Switzerland) or a BioTek Epoch 2 plate reader (BioTek Instruments), maintained at 37°C. Growth (OD600) was monitored following a kinetic cycle consisting of 12 shaking steps, alternating between linear and orbital movements (with 1 or 2 mm amplitude), each lasting 60 s. OD measurements obtained from the plate reader were calibrated to correspond with those from a standard cuvette, establishing a correlation where ODcuvette = ODplate/0.23. All growth experiments were carried out in duplicate or triplicate when indicated.

Adaptive laboratory evolution of pre-2KG-aux strain

In growth experiment testing 2KG production via alternative 2KG biosynthesis, some strains grew after 80 h under conditions where ethylene glycol was present at >50 mM concentration (Supplementary Fig S3 and S4). These strains were re-inoculated 1:100 dilution in selective M9 minimal media with 14 mM pyruvate, 10.5 mM succinate, and 50 mM ethylene glycol. After growth was observed on the following day, the strains were re-inoculated in the same media. The procedure was repeated three times. The DNA of the resulting cultures was isolated and sent for whole-genome sequencing analysis together with the DNA of their respective parental strains.

Whole-genome sequencing and analysis

NucleoSpin Microbial DNA kit (MACHERY-NAGEL, Düren, Germany) was used for genomic DNA extraction following manufacturer's instructions. Library construction used Nextera XT kit (Illumina) and genome sequencing was on a paired-end Illumina sequencing platform MiSeq. Raw reads have been deposited at the NCBI Sequence Read Archive (SRA) and can be accessed under BioProject PRJNA1133637. The sequencing data were first passed through quality trimming using BBduk (v38.84), then mapped to a MG1655 *in silico* modified with genomic insertion of *Cc_xylXA* as reference genome using breseq (v0.36.1) or Genious Prime (v20231.2).

Results

Design of auxotrophic strategies for GA-biosensing in *E. coli*

In our study, we aimed to use *E. coli* as platform to establish our GA biosensors. Given that GA is a non-essential metabolite, we thought of creating artificial metabolic dependencies, i.e. auxotrophies that would allow us to couple GA detection to growth of in *E. coli*. In a first approach, we chose PLP, one of the vitamin B6 vitamers, as target molecule to create an artificial auxotrophy. PLP is an essential cofactor utilized by at least 60 enzymes in *E. coli*, including transaminases and amino acid decarboxylases. Notably, PLP can be derived from GA via an alternative PLP synthesis pathway [21–23] (Fig. 1). This pathway, present in *E. coli*, begins with the aldol condensation of GA and glycine, catalyzed by the low-specific threonine aldolase (LtaE), to produce 4-hydroxythreonine [23]. This compound is then phosphorylated by homoserine kinase (ThrB) to generate L-4-phospho-hydroxythreonine, an intermediate metabolite in canonical PLP biosynthesis pathway. Finally,

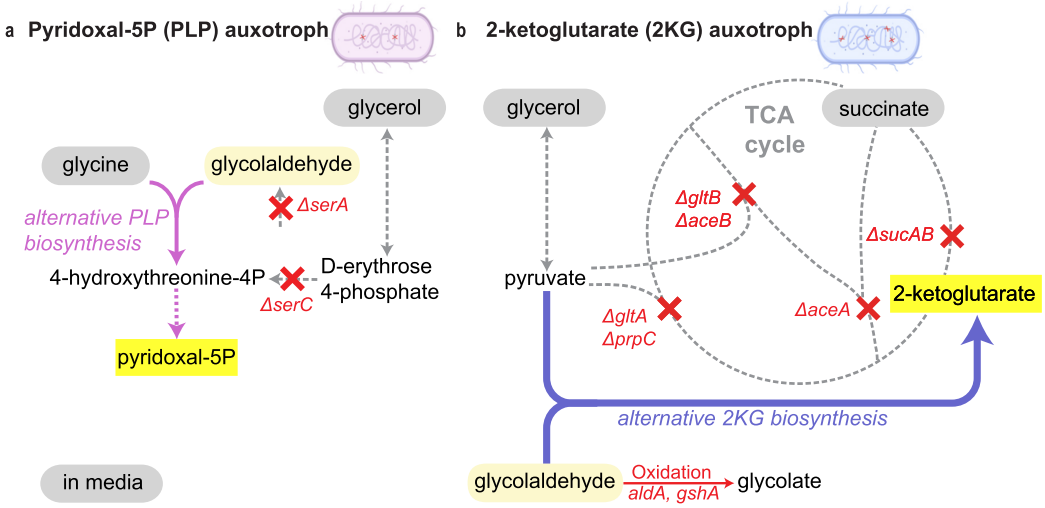

Figure 2. Glycolaldehyde biosensors constructed in this study. (a) PLP-aux strain. Δ*serC* causes an auxotrophy for essential metabolite PLP (highlighted in yellow), whereas Δ*serA* avoids intracellularly produced glycolaldehyde. (b) 2KG-aux strain. Δ*aceAB*, Δ*glcB*, Δ*gltA*, Δ*sucAB*, and Δ*prpC* deletions isolate 2KG segment of TCA cycle from rest of metabolism and create 2KG auxotrophy. GA sinks are indicated under "oxidation" caption).

three further enzymatic steps lead to PLP production (Supplementary Fig. S1).

In an alternative approach, we selected 2KG as target for auxotrophy in the development of a second type of GA biosensor. 2KG is an essential metabolite for amino acid biosynthesis and is intricately involved in the tricarboxylic acid cycle (TCA) within *E. coli*. This choice marks a significant divergence from the PLP biosensor, primarily due to the increased amounts of 2KG required for bacterial growth compared to PLP. The challenge then lies in connecting the production of 2KG using GA as a precursor. We combined elements of Dahms and Weimberg pathways, utilizing three enzymatic steps, to bridge this gap. The final reaction of the Dahms pathway involves the aldolase cleavage of 2-keto-3-deoxy-D-xylonate into pyruvate and GA [24]. We reasoned that this reaction could be reversed to synthesize the C5 compound from GA and pyruvate, which could then be converted to 2KG via the last two steps of the Weimberg pathway [25], achieving an alternative biosynthesis pathway for 2KG (Fig. 1).

Beyond expanding the range of sensitivity over a range of GA concentrations, establishing two types of GA biosensors with contrasting GA requirements also allows to use these strains in selection schemes with increasing selection pressure for GA producing pathways.

Construction and optimization of the *E. coli* GA-biosensors

To realize the auxotrophic schemes, we engineered the metabolic network of *E. coli* to rely on the two different biosynthetic routes, creating two distinct biosensors for GA detection. The first approach involved truncating canonical PLP biosynthesis (Supplementary Fig. S1) by deleting the gene-encoding phosphoserine/phosphohydroxythreonine aminotransferase (Δ*serC*). This deletion prevented the formation of the PLP precursor (4-hydroxythreonine-4P) from erythrose 4-P. Additionally, to decrease endogenous GA production through other pathways, which could potentially interfere with sensitivity of the biosensor, we removed phosphoglycerate dehydrogenase (Δ*serA*). The absence of this enzyme prevents the formation of 3-phosphohydroxypyruvate, a precursor to 3-hydroxypyruvate, which can spontaneously decarboxylate into GA [23].

We tested the resulting PLP-auxotrophic strain (PLP-aux; Fig. 2a) for growth with externally added pyridoxine or GA on minimal medium, which validated growth dependency on these two compounds. We also assessed the growth responses of PLP-aux across a gradient of GA concentrations, from micromolar to millimolar levels, which revealed a clear correlation between the maximum optical density (OD_{600}) of the culture and the GA concentration of the medium, establishing the PLP-aux strain as GA biosensor (Fig. 3).

For our second GA biosensor, we engineered a strain of *E. coli* to become auxotrophic for 2KG by selectively targeting and deleting genes linked to the tricarboxylic acid (TCA) cycle and related metabolic routes. These deletions included enzymes that contribute to 2KG consumption (Δ*sucA* and Δ*sucB*), citrate synthase activity (Δ*gltA* and Δ*prpC*), and glyoxylate metabolism (Δ*glcBDEFG*, Δ*aceK*, Δ*ghrA*, Δ*ghrB*, and Δ*aceB*), making the strain dependent on external 2KG sources (Supplementary Fig. S2).

To facilitate the synthesis of 2KG from GA and pyruvate, we incorporated elements from the Dahms and Weimberg pathways, which are naturally absent in *E. coli*. We identified two *E. coli* genes, *yagE* and *yjhH*, capable of catalyzing the initial aldolase reaction required for GA and pyruvate condensation [3]. For the subsequent steps, we tested different candidate genes reported in the literature (Supplementary Fig. S3), and employed genes from the Weimberg pathway operon (*xylXABCD*) from *C. crescentus* (Stephens et al., 2007). Specifically, we introduced *Cc_xylX* (2-keto-3-deoxyxylonate dehydratase) and *Cc_xylA* (2-ketoglutarate semialdehyde dehydrogenase) into the genome of one of the strains that underwent a short adaptive laboratory evolution (Supplementary Fig. S4). The strain obtained exhibited a truncated *xynR* gene, which has been previously reported to act as a repressor of the *yagE* gene [26]. This genetic modification resulted in the 2KG-aux strain. This strain is able to relieve its auxotrophy by the conversion of GA to 2KG (Fig. 2b).

Similar to the first biosensor, we assessed growth of the 2KG-aux strains across a range of GA concentrations (20 μM—1.5 mM) in minimal medium supplemented with glycerol and succinate. Again, maximal OD_{600}, correlated well with the GA concentration (Fig. 3). Compared to the PLP-aux strain, the 2KG-aux

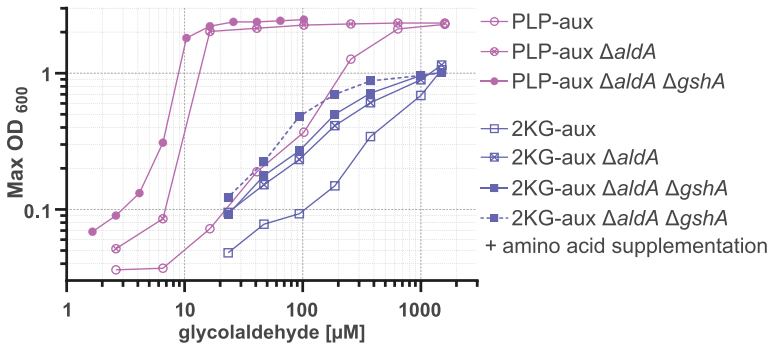

Figure 3. Sensitivity of glycolaldehyde biosensors. Maximal OD_{600} as function of concentrations of glycolaldehyde tested in the PLP-aux and 2KG-aux strains. Gene deletions for GA oxidation deleted individually (Δ*aldA*) or combined (with Δ*gshA*). Improvement in sensitivity via amino acid supplementation was also tested in the 2KG-aux strain (see text for details). Values shown for each data point represent the average of the technical replicates ($n = 2$).

strain reached lower maximal OD_{600} and showed a slightly lower dynamic range across the range of concentrations tested.

To enhance the sensitivity of our GA biosensors, we searched for internal metabolic pathways that could divert GA, which would negatively affect its detection. We identified several routes, including the oxidation of GA to glycolate by aldehyde dehydrogenase (AldA), GA scavenging by glutathione, and reduction of GA to ethylene glycol primarily by aldehyde reductase (YqhD), among other aldehyde reductases [27–29]. Having identified these potential GA sinks, we proceeded with combinatorial gene deletions targeting these routes. Starting with the PLP-aux strain, we executed deletions of Δ*aldA*, Δ*gshA* (which encodes glutamate-cysteine ligase and was targeted to prevent the creation of glutathione), Δ*yqhD* and the combined deletion of aldehyde reductases: Δ*yahK*, Δ*gldA*, Δ*dkgA*, Δ*yghA*, Δ*fucO*, Δ*eutG*, Δ*ybbO*, Δ*adhE*, Δ*yjgB*, Δ*adhP*, and Δ*adhE*. Collectively, these gene deletions aimed to enhance the responsiveness of the strain to GA.

Upon testing the modified PLP-aux strain across a range of GA concentrations (2 μM—1.2 mM) in minimal medium supplemented with glycerol and glycine, we observed significant improvements in sensitivity. The deletion of Δ*aldA* notably enhanced the maximal OD_{600} of the strain in response to GA. An additive effect was observed, when Δ*aldA* was combined with Δ*gshA* (Fig. 3). However, deleting Δ*yqhD* and other reductases yielded minimal to no sensitivity improvements (Supplementary Fig. S5).

Building on these findings, we applied the most impactful deletion, Δ*aldA*, and its combination with Δ*gshA*, also to the 2KG-auxotrophic strain. Assessing growth across various GA concentrations (20 μM—1.5 mM) in minimal medium with glycerol and succinate confirmed improved GA sensitivity for both strains (Fig. 3). Additionally, to alleviate selection pressure on the 2KG-aux strain, we explored supplementing amino acids derived from 2KG, which would not relieve the auxotrophy [30]. Our experiments included alanine, aspartate, isoleucine, leucine, phenylalanine, serine, tyrosine, and valine, none of which alleviated the auxotrophy, but some (aspartate, isoleucine, phenylalanine, and serine) enhanced final biomass yield or doubling time (Supplementary Fig. S6). When comparing the maximal OD_{600} of the amino acid-supplemented strains (aspartate, isoleucine, phenylalanine and serine), with the non-supplemented strain, we saw an increased maximal OD_{600} below GA concentrations of 600 μM (Fig. 3).

Based on these results, we decided to continue our experiments with the PLP-aux Δ*aldA* strain. This strain reached its maximal optical density at a GA concentration of ~20 μM, reflecting its high sensitivity to GA, as it responded robustly to lower concentrations compared to other strains, while maintaining a functional glutathione biosynthesis operon. While knocking out glutathione biosynthesis seemed not to be lethal and even increased GA sensitivity slightly in PLP-aux Δ*aldA* (Fig. 3), the advantages did not seem to outweigh the potential drawbacks. Glutathione plays critical roles beyond the scope of this experiment, such as regulating intracellular pH through potassium (K^+) concentrations and providing protection against a variety of toxic compounds [31]. Therefore, we concluded that maintaining its biosynthesis would benefit the overall robustness and efficiency of the strain. In addition, we also engineered the strain to constitutively overexpress homoserine kinase ThrB, which catalyzes an irreversible step in PLP synthesis. The rationale behind increasing ThrB expression was to not bottleneck the aldolase reaction and increase flux through the system.

Having established a highly sensitive biosensor with PLP-aux Δ*aldA*, we opted for a less sensitive 2KG-aux GA sensor, for which we returned to the initial strain design (without Δ*aldA* and Δ*gshA*). This allowed us to operate selection at very high fluxes and demand for high GA concentrations for OD_{600} readout.

Biosensing intracellular GA-producing pathways

We next evaluated our GA biosensors for detecting intracellular GA produced through various metabolic pathways. We selected three different pathways that utilized different starting substrates and involved different natural and new-to-nature enzymes: (I) ethylene glycol oxidation to GA facilitated by overexpressing the native L-lactaldehyde dehydrogenase (*fucO*) of *E. coli*; (II) xylose catabolism into GA and pyruvate via the Dahms pathway with an overexpressed heterologous operon from *C. crescentus*; and (III) a new-to-nature glycolate reduction route that provides GA via two engineered enzymes (Fig. 4).

We first assessed a pathway naturally occurring in *E. coli* that can produce GA using endogenous genes. To that end, we examined L-1,2-propanediol oxidoreductase (FucO), an Fe^{2+}-dependent enzyme known for its role in L-fucose or LL-rhamnose fermentation pathways, which is documented to facilitate the oxidation of ethylene glycol to GA in *E. coli* [32]. As all of our assays were performed aerobically, we used a mutant FucO variant (I7L L8V) that shows higher oxygen-tolerance compared to the wild-type [20]. Overexpressing FucO indeed allowed the bacteria to sense the conversion from ethylene glycol toward GA, illustrating its capability

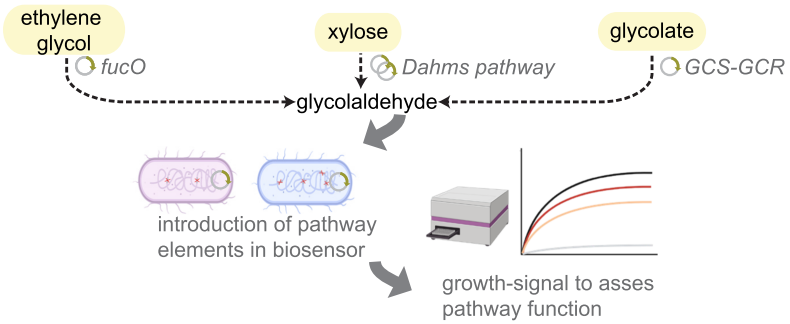

Figure 4. Biosensor workflow. After constructing vectors expressing elements for a glycolaldehyde producing pathway, they can be tested in one of the engineered strains from this study. Bacterial growth is used as read out for pathway operation. Enzymes used in this study: L-1,2-propanediol oxidoreductase (*fucO*) from *E. Coli*; Engineered enzymes glycolyl-CoA synthetase (GCS) and glycolyl-CoA reductase (GCR) [8].

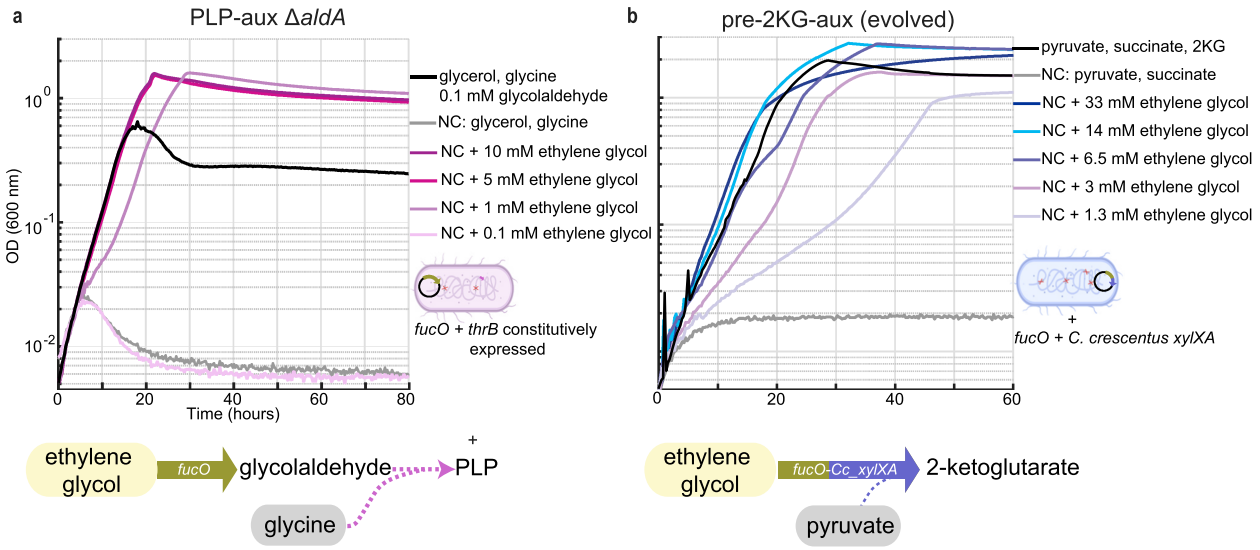

Figure 5. Ethylene glycol oxidation detected in glycolaldehyde biosensors. (a) Growth of the PLP-aux Δ*aldA* strain with the overexpression of L-1,2-propanediol oxidoreductase *fucO* in M9 minimal media with 20 mM glycerol, 4 mM glycine (NC), or with the addition of 0.1 mM glycolaldehyde or varying ethylene glycol concentrations. (b) Evolved pre-2KG-aux strain relieves auxotrophy via the oxidation of ethylene glycol to glycolaldehyde with overexpression of *fucO* and *C. crescentus* genes *Cc_xylXA* for its subsequent conversion to 2KG in M9 minimal media with 14 mM glycerol, 10.5 mM succinate (NC), or with the addition of 1 mM 2KG or varying ethylene glycol concentrations. Lines represent mean values of technical replicates. ($n = 2$).

to detect intracellularly produced GA (Fig. 5a), while the empty vector did not exhibit growth in ethylene glycol (Supplementary Fig. S7a).

Similarly, we aimed to evaluate the ability of the alternative GA biosensor (with 2KG auxotrophy) to detect GA produced *in vivo* by overexpressing FucO and utilizing ethylene glycol as the GA source. The initial tests for this purpose employed a predecessor of the 2KG-aux strain (pre-2KG-aux). This strain anteceded the genomic integration of the *Cc_xylXA* genes. Instead, they were overexpressed alongside with *fucO* from a plasmid. The initial experiment demonstrated that the strain exhibited sporadic relief from its auxotrophy following a lag phase, and only under high ethylene glycol concentrations (>35 mM) (Supplementary Fig. S3c). This result indicated that some adaptation was required before growth could be achieved. Consequently, the growing strain was re-isolated and subjected to a further short adaptive laboratory evolution. Following three re-inoculations of the strain in minimal containing ethylene glycol, a mutation was identified within the DNA-binding domain of the transcriptional repressor of the *yagEF* operon (*xynR*) (Supplementary Fig. S4a). Overexpression of FucO also enabled the pre-2KG-aux strain to detect intracellularly produced GA from externally added ethylene glycol (Fig. 5b). Plasmid curing again abolished growth of the strain in presence of ethylene glycol, confirming the dependency on FucO (Supplementary Fig. S7b).

While both GA biosensor strains, PLP-aux and 2KG-aux, were principally suited to detect intracellularly produced GA, the PLP-aux strain was more sensitive at lower ethylene glycol concentrations (Fig. 5).

Dahms and Weimberg pathway in biosensors

After successfully demonstrating the capability of our strains to sense single-step enzymatic conversions to GA, we explored the feasibility of more complex, multistep reactions producing GA *in vivo*. We focused on the Dahms pathway, which is known for converting xylose into GA [24]. This pathway has been previously introduced in *E. coli* to produce various chemicals such as glycolic acid, lactic acid, and 1,4 butanediol [33–37].

We assessed whether one of our PLP-aux strains could detect GA produced through the heterologous expression of enzymes from this pathway. We constructed an expression vector containing the *C. crescentus* operon (*Cc_xylBCD*) responsible for converting xylose into 2-keto-3-deoxy-D-xylonate, and introduced it into the PLP-aux Δ*aldA* strain. This vector, combined with endogenous *E.*

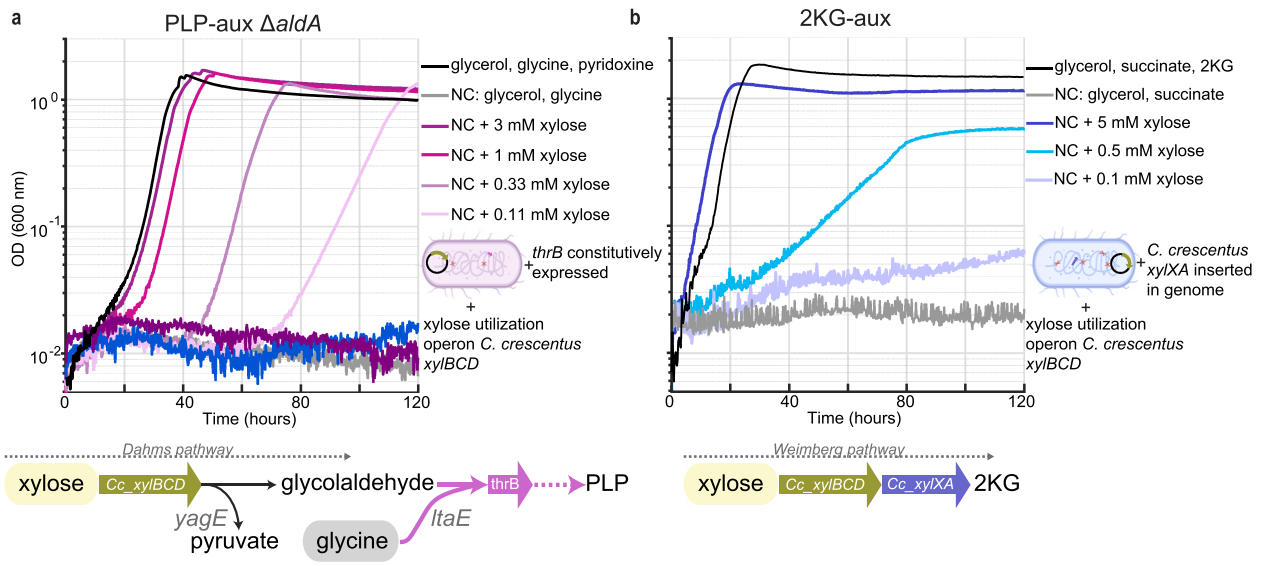

Figure 6. Dahms and Weimberg pathway restores growth in biosensors. (a) Growth of PLP-aux Δ*aldA* strain overexpressing *Cc_xylBCD* from a plasmid in M9 minimal medium containing 20 mM glycerol and 4 mM glycine (NC), or with the addition of 80 μM pyridoxine or varying concentrations of xylose. Irreversible reaction by homoserine kinase (ThrB) overexpression from genome to drive PLP biosynthesis. (b) Growth of 2KG-aux strain harboring all genes for Weimberg's pathway from *C. crescentus* in M9 minimal medium with 14 mM glycerol and 10 mM succinate (NC), or with the addition of 1 mM 2KG or varying concentrations of xylose. Lines represent mean values of technical replicates. ($n = 2$).

coli genes *yagE* and *yjhH*, effectively replicated the Dahms pathway, and enabled growth of the biosensor with xylose as GA source. Growth characterization in minimal medium confirmed that xylose could alleviate PLP auxotrophy similar to the response with pyridoxine (Fig. 6a). To elucidate which endogenous gene from *E. coli* primarily drives the final reaction of the Dahms pathway, we repeated the experiment using strains with additionally deletions of Δ*yagE* or Δ*yjhH*. The strain lacking *yagE* exhibited no growth in the presence of xylose, indicating that YagE catalyzes the final reaction of the Dahms pathway in *E. coli* (Supplementary figure S8).

For the 2KG-aux strain, we additionally explored the possibility of direct (i.e. GA-independent) sensing of xylose through the Weimberg pathway that converts xylose into 2KG [25]. This pathway, previously introduced in *E. coli* for production of poly-3-hydroxybutyrate [38], does not involve GA as intermediate, but still provides 2KG as end product. The Weimberg pathway shares the initial three catalytic steps with the Dahms pathway, which yield 2-keto-3-deoxy-D-xylonate, and which we had already confirmed *in vivo* (see above). The remaining enzymatic steps in the Weimberg pathway consist in the dehydration and oxidation of 2-keto-3-deoxy- D-xylonate to 2KG. These are precisely the steps we employed in this study to convert the 2KG-aux into a GA sensor (*Cc_xylXA*; Fig. 1). We introduced the plasmid for xylose utilization (*Cc_xylBCD*) into the 2KG-aux strain with *Cc_xylXA* genomically integrated. Testing different xylose supplementation showed xylose-dependent (and GA-independent) growth of 2KG-aux biosensor (Fig. 6b), demonstrating a general flexibility of the 2KG-aux strain for additional biosensing applications.

New-to-nature glycolate reduction to GA restores growth in PLP-aux strain

We finally progressed to using our biosensors to confirm the *in vivo* functionality of a new-to-nature enzyme cascade constructed from engineered enzymes. As mentioned earlier, Trudeau et al. recently conceived a new-to-nature route for the reduction of glycolate into GA, employing two engineered enzymes, GCS and GCR. To date, these enzymes had been exclusively utilized *in vitro* to assess their catalytic efficiencies and substrate specificities, but so far not confirmed *in vivo* [8,9].

We expressed GCS GCR in the PLP-aux strain, but initially failed to observe growth on minimal medium with glycolate supplementation (data not shown), indicating that the activity of GCS and/or GCR was not sufficient to provide sufficient GA for growth. We thus switched to the PLP-aux Δ*aldA* strain with constitutively expressed *thrB*, which has a higher GA sensitivity (Fig. 3). We further noted that GCS is post-translationally inactivated through acetylation of an active site lysine by *E. coli* lysine acetylase [9]. We deleted the gene-encoding lysine acetylase (Δ*patZ*) to prevent inactivation of the GCS enzyme and also knocked out isocitrate lyase (Δ*aceA*) to block glycolate production from glyoxylate (Fig. 7a).

These genetic modifications indeed restored glycolate-dependent growth, confirming the *in vivo* functionality of the glycolate reduction pathway (Fig. 7b). We next sought to replace GCS by a promiscuous CoA transferase (*abfT*) from *C. aminobutyricum*. This also supported growth upon the addition of glycolate, albeit with an extended lag phase compared to the GCS variant of the pathway (Fig. 7b). In contrast, the strain without an expression vector was not able to relief its auxotrophy in presence of glycolate (Supplementary figure S9). Overall, this data did not only provide proof for the reductive conversion of glycolate to GA *in vivo*, but also allowed to directly assess performance of different pathways designs (glycolyl-CoA synthetase versus CoA transferase) within the cell. Efforts to extend these findings to our second GA biosensor, failed, as the flux through either cascade was insufficient to feed the high biomass demand of the 2KG biosensor (data not shown).

Discussion

Here, we present two new GA sensors with different metabolic architectures and sensitivities. The PLP-aux strain detects GA by

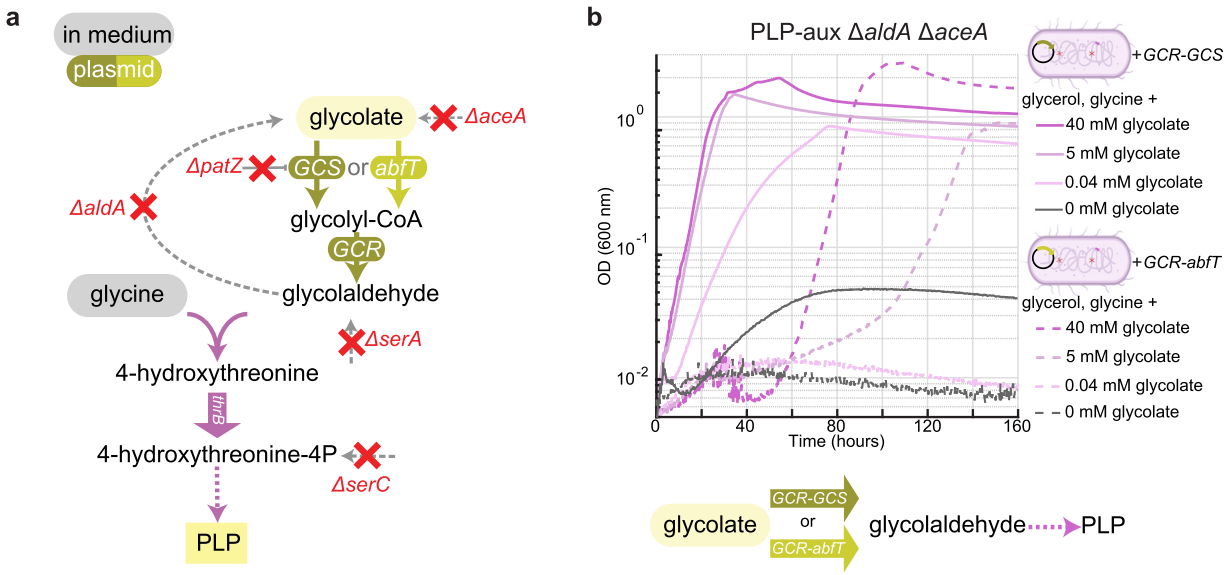

Figure 7. New-to-nature glycolate reduction in PLP-aux strain. (a) Schematic illustration of the PLP-aux strain with an expression vector coding for enzymes required for glycolate reduction: GCS: glycolyl-CoA synthetase or abfT: 4-hydroxybutyrate CoA-transferase from *Clostridium aminobutyricum* and GCR: glycolyl-CoA reductase. ΔserA and ΔserC cause an auxotrophy for pyridoxal-5P. ΔaldA and ΔaceA were introduced in order to avoid undesired sinks or sources of pathway intermediates. ΔpatZ was introduced to avoid GCS repression. thrB is constitutively overexpressed from the genome. (b) *In vivo* new-to-nature reduction of glycolate to glycolaldehyde via different enzymes. M9 minimal medium containing 20 mM glycerol and 4 mM glycine with different concentrations of glycolate. Lines represent mean values of technical replicates. ($n = 3$).

growth dependence on GA-dependent biosynthesis of the essential cofactor PLP. The 2KG-aux strain reverses the last reaction of the Dahms pathway, followed by the last two steps of the Weimbergs pathway, establishing a new pathway leading to GA-dependent biosynthesis of 2KG.

Our study showcases the power of metabolic engineering in crafting innovative biosensors, in particular the designing of auxotrophic strategies for detecting non-essential metabolites. In contrast to the limited operational range of 1–10 mM from the previously reported promiscuous aldehyde biosensors [10], our sensor strains exhibit a substrate-specific (i.e. GA-specific) response, covering a sensitivity range spanning three orders of magnitude (μM-mM) toward GA. The most sensitive variant of the PLP-aux strain here presented shows a growth phenotype with concentrations as low as ~4 μM of GA.

By introducing additional knock outs (e.g. *aldA*, *gshA*) and supplementing different amino acids in the medium, we further improved sensitivity of the GA biosensors. In case of 2KG, supplementation of serine, asparte, isoleucine, and phenylalanine decreased the amount of 2KG required for growth. Note that these amino acids have been reported to serve as (alternative) ammonium sources to glutamate (and glutamine), which is typically the main source for ammonium and serves as nitrogen acceptor/donor in transaminase reactions [30, 39]. Since glutamate is directly derived from 2KG, addition of abovementioned amino acids might reduce the glutamate requirements to meet this demand and thus alleviate the selection pressure.

Importantly, as growth of the strain is the read out signal of the biosensor, no specialized equipment, such as fluorescence detection is required, which makes our strains convenient tools for assessing and fine-tuning natural or synthetic pathways that produce GA, as well as for detecting intermediates of the GA-dependent pathways that alleviate the engineered auxotrophies. Potential challenges, such as contamination by wild-type strains, can be effectively mitigated by including antibiotics in the media, leveraging the resistance cassette used during genetic manipulation of the strain. Furthermore, our biosensors offer additional advantages. Given that all modifications were done at the genomic level, their plasmid-free nature ensures stability and reduces the risk of genetic drift, which makes them ideal platforms for adaptive laboratory evolution experiments [18]. By providing two sensor strains with varying degrees of GA dependence, a broader dynamic range of detection is achieved compared to a single sensor. For example, in our ethylene glycol experiments, the highly sensitive PLP-auxotroph may saturate quickly and fail to distinguish between different ethylene glycol concentrations, while the 2KG-auxotroph can still detect variations. On the contrary, for our synthetic glycolate reduction pathway, the (modified) PLP-aux strain was just sensitive enough to pick up GA formation *in vivo*, while the 2KG-aux strain was too insensitive at this stage. Overall, this multisensor approach ensures coverage of a wide range of GA levels, which becomes crucial and helpful, when the output of new pathways or enzyme variants is unknown.

Other studies have effectively made use of auxotrophy-based biosensors for other metabolites such as glycerate, formaldehyde, oxaloacetate, aspartate, intermediates of the pentose phosphate pathway, or even other cofactors such as NADH [40–44] and their importance is highlighted for optimizing novel activities *in vivo* [45]. By expanding the repertoire of engineered biosensors, this study lays the groundwork for prospective applications in biotechnology and synthetic biology.

Acknowledgments

The authors would like to thank Beau Dronsella and Ari Satanowsky for helpful discussions and feedback on the manuscript.

Supplementary data

Supplementary data is available at *SYNBIO* online

Conflict of interest: None declared.

Funding

This Project was funded by Max Planck society general funding and EU's Horizon 2020 research and innovation programme under the Grant Agreement 862087.

Data availability

Raw reads of sequencing data are deposited at NCBI and can be accessed under BioProject: PRJNA1133637. The data underlying this article is available in FigShare at https://figshare.com/projects/Two_highly_specific_growth-coupled_biosensor_for_glycolaldehyde_detection_across_M_and_mM_concentrations/223221. Plasmids were deposited within Genebank: Submission # 2578076.

References

1. Riha WE, Wendorff WL. Browning potential of liquid smoke solutions: comparison of two methods. *J Food Sci* 1993;**58**:671–74.
2. Faveere W, Mihaylov T, Pelckmans M *et al*. Glycolaldehyde as a bio-based c2 platform chemical: catalytic reductive amination of vicinal hydroxyl aldehydes. *ACS Catal* 2020;**10**:391–404.
3. Liu H, Ramos KRM, Valdehuesa KNG *et al*. Biosynthesis of ethylene glycol in Escherichia coli. *Appl Microbiol Biotechnol* 2013;**97**:3409–17.
4. Zhou J, Tian X, Yang Q *et al*. Three multi-enzyme cascade pathways for conversion of C1 to C2/C4 compounds. *Chem Catal* 2022.
5. Ru J, Huo Y, and Yang Y. Microbial degradation and valorization of plastic wastes. *Front Microbiol* 2020;**11**:442.
6. Lu X, Liu Y, Yang Y *et al*. Constructing a synthetic pathway for acetyl-coenzyme A from one-carbon through enzyme design. *Nat Commun* 2019;**10**:1–10.
7. Mao Y, Yuan Q, Yang X *et al*. Non-natural Aldol Reactions Enable the Design and Construction of Novel One-Carbon Assimilation Pathways in vitro. *Front Microbiol* 2021;**12**:677596.
8. Trudeau DL, Edlich-Muth C, Zarzycki J *et al*. Design and in vitro realization of carbon-conserving photorespiration. *Proc Natl Acad Sci U S A* 2018;**115**:E11455–64.
9. Scheffen M, Marchal DG, Beneyton T *et al*. A new-to-nature carboxylation module to improve natural and synthetic CO2 fixation. *Nat Catal* 2021;**4**:105–15.
10. Frazão CR, Maton V, François JM *et al*. Development of a metabolite sensor for high-throughput detection of aldehydes in Escherichia coli. *Front Bioeng Biotechnol* 2018;**6**:1–12.
11. Orsi E, Claassens NJ, Nikel PI *et al*. Growth-coupled selection of synthetic modules to accelerate cell factory development. *Nat Commun* 2021;**12**:1–5.
12. Jensen SI, Lennen RM, Herrgard MJ *et al*. Seven gene deletions in seven days: fast generation of Escherichia coli strains tolerant to acetate and osmotic stress. *Sci Rep* 2015;**5**:17874.
13. Braatsch S, Helmark S, Kranz H *et al*. Escherichia coli strains with promoter libraries constructed by Red/ET recombination pave the way for transcriptional fine-tuning. *Biotechniques* 2008;**45**:335–37.
14. Datsenko KA, Wanner BL. One-step inactivation of chromosomal genes in Escherichia coli K-12 using PCR products. *Proc Natl Acad Sci U S A* 2000;**97**:6640–45.
15. Baba T, Ara T, Hasegawa M *et al*. Construction of Escherichia coli K-12 in-frame, single-gene knockout mutants: the Keio collection. *Mol Syst Biol* 2006;**2**:2006.0008.
16. Thomason LC, Costantino N, Court DLE. Coli genome manipulation by P1 transduction. *Curr Protoc Mol Biol* 2007;**79**:1.17.1–1.17.8.
17. Bassalo MC, Garst AD, Halweg-Edwards AL *et al*. Rapid and efficient one-step metabolic pathway integration in E. coli. *ACS Synth Biol* 2016;**5**:561–68.
18. Wenk S, Yishai O, Lindner SN *et al*. An engineering approach for rewiring microbial metabolism. *Methods Enzymol* 2018;**608**:329–367.
19. Grote A, Hiller K, Scheer M *et al*. JCat: a novel tool to adapt codon usage of a target gene to its potential expression host. *Nucleic Acids Res* 2005;**33**:526–31.
20. Lu Z, Cabiscol E, Obradors N *et al*. Evolution of an Escherichia coli protein with increased resistance to oxidative stress. *J Biol Chem* 1998;**273**:8308–16.
21. Eliot AC, Kirsch JF. Pyridoxal phosphate enzymes: mechanistic, structural, and evolutionary considerations. *Annu Rev Biochem* 2004;**73**:383–415.
22. Hayashi H. Pyridoxal enzymes: mechanistic diversity and uniformity. *J Biochem* 1995;**118**:463–73.
23. Kim J, Kershner JP, Novikov Y *et al*. Three serendipitous pathways in E. coli can bypass a block in pyridoxal-5′-phosphate synthesis. *Mol Syst Biol* 2010;**6**:436.
24. Dahms AS, Anderson RL. 2-Keto-3-deoxy-L-arabonate aldolase and its role in a new pathway of L-arabinose degradation. *Biochem Biophys Res Commun* 1969;**36**:809–14.
25. Weimberg R. Pentose oxidation by Pseudomonas fragi*. *J Biol Chem* 1961;**236**:629–35.
26. Shimada T, Momiyama E, Yamanaka Y *et al*. Regulatory role of XynR (YagI) in catabolism of xylonate in Escherichia coli K-12. *FEMS Microbiol Lett* 2017;**364**:1–9.
27. Jayakody LN, Kadowaki M, Tsuge K *et al*. SUMO expression shortens the lag phase of Saccharomyces cerevisiae yeast growth caused by complex interactive effects of major mixed fermentation inhibitors found in hot-compressed water-treated lignocellulosic hydrolysate. *Appl Microbiol Biotechnol* 2015;**99**:501–15.
28. Alkim C, Cam Y, Trichez D *et al*. Optimization of ethylene glycol production from (d)-xylose via a synthetic pathway implemented in Escherichia coli. *Microb Cell Fact* 2015;**14**:127.
29. Rodriguez GM, Atsumi S. Toward aldehyde and alkane production by removing aldehyde reductase activity in Escherichia coli. *Metab Eng* 2014;**25**:227–37.
30. Schulz-Mirbach H, Müller A, Wu T *et al*. On the flexibility of the cellular amination network in E. coli. *Elife* 2022;**11**:1–42.
31. Ferguson GP, Booth IR. Importance of glutathione for growth and survival of Escherichia coli cells: detoxification of methylglyoxal and maintenance of intracellular K+. *J Bacteriol* 1998;**180**:4314–18.
32. Boronat A, Caballero E, Aguilar J. Experimental evolution of a metabolic pathway for ethylene glycol utilization by Escherichia coli. *J Bacteriol* 1983;**153**:134–39.
33. Cabulong RB, Lee W, Bañares AB *et al*. Engineering Escherichia coli for glycolic acid production from D-xylose through the Dahms pathway and glyoxylate bypass. *Appl Microbiol Biotechnol* 2018;**102**:2179–89.
34. Chae TU, Ryu JY, Ryu JY. Production of ethylene glycol from xylose by metabolically engineered Escherichia coli. *AIChE J* 2018;**64**:4193–200.
35. Choi SY, Kim WJ, Yu SJ *et al*. Engineering the xylose-catabolizing Dahms pathway for production of poly(d -lactate- co -glycolate) and poly(d -lactate- co -glycolate- co - d –2-hydroxybutyrate) in Escherichia coli. *Microb Biotechnol* 2017;**10**:1353–64.
36. Fujiwara R, Noda S, Tanaka T *et al*. Metabolic engineering of Escherichia coli for shikimate pathway derivative production from. *Nat Commun* 2020;**11**:1–7.
37. Salusjärvi L, Havukainen S, Koivistoinen O *et al*. Biotechnological production of glycolic acid and ethylene glycol: current state and perspectives. *Appl Microbiol Biotechnol* 2019;**103**:2525–35.

38. Shi LL, Zheng Y, Tan BW *et al*. Establishment of a carbon-efficient xylulose cleavage pathway in Escherichia coli to metabolize xylose. *Biochem Eng J* 2022;**179**:108331.
39. Yang Z, Han Y, Ma Y *et al*. Global investigation of an engineered nitrogen-fixing Escherichia coli strain reveals regulatory coupling between host and heterologous nitrogen-fixation genes. *Sci Rep* 2018;**8**:1–13.
40. Aslan S, Noor E, Benito S *et al*. Design and engineering of E. coli metabolic sensor strains with a wide sensitivity range for glycerate. *Metab Eng* 2020;**57**:96–109..
41. Schann K, Bakker J, Boinot M *et al*. Design, construction and optimization of formaldehyde growth biosensors with broad application in Biotechnology. *bioRxiv* 2023. 10.1101/2023.06.29.547045
42. Schada von Borzyskowski L, Schulz-Mirbach H, Troncoso Castellanos M *et al*. Implementation of the β-hydroxyaspartate cycle increases growth performance of Pseudomonas putida on the PET monomer ethylene glycol. *Metab Eng* 2023;**76**: 97–109.
43. Wu T, Gómez-Coronado PA, Kubis A *et al*. Engineering a synthetic energy-efficient formaldehyde assimilation cycle in Escherichia coli. *Nat Commun* 2023;**14**:8490.
44. Wenk S, Schann K, He H *et al*. An energy-auxotroph Escherichia coli provides an in vivo platform for assessing.pdf. *Biotechnol Bioeng* 2020;**117**:3233–606.
45. Schulz-Mirbach H, Dronsella B, He H *et al*. Creating new-to-nature carbon fixation: A guide. *Metab Eng* 2024;**82**:12–28.

Synthetic Biology, 2025, 10(1), ysaf004 , DOI: https://doi.org/10.1093/synbio/ysaf004, Advance Access Publication date: 4 April 2025, Research Article
Submitted: 27 February 2025; **Received (in revised form)**: 30 January 2025; **Accepted**: 3 April 2025